

**THEORETICAL CONSTRAINTS IN THE DESIGN OF
MULTIVARIABLE CONTROL SYSTEMS**

**PROGRESS REPORT FOR PERIOD
1 JULY 1992 - 1 SEPTEMBER 1992**

NASA GRANT NO. NAG1-1361

(NASA-CR-191943) THEORETICAL
CONSTRAINTS IN THE DESIGN OF
MULTIVARIABLE CONTROL SYSTEMS
Progress Report, 1 Jul. - 1 Sep.
1992 (Calspan-State Univ. of New
York Joint Venture) 30 p

N93-16383

Unclass

G3/61 0141240

PREPARED BY:

**CALSPAN-UB RESEARCH CENTER
P.O. BOX 400
BUFFALO, NY 14225**

**MR. E. G. RYNASKI
DR. D. JOSEPH MOOK
MR. JUAN DEPEÑA**

PROGRAM DESCRIPTION

The research being performed under NASA Grant NAG1-1361 involves a more clear understanding and definition of the constraints involved in the pole-zero placement or assignment process for multiple input, multiple output systems. Complete state feedback to more than a single controller under conditions of complete controllability and observability is redundant if pole placement alone is the design objective. The additional feedback gains, above and beyond those required for pole placement can be used for eigenvalue assignment or zero placement of individual closed loop transfer functions. Because both poles and zeros of individual closed loop transfer functions strongly affect the dynamic response to a pilot command input, the pole-zero placement problem is important.

When fewer controllers than degrees of freedom of motion are available, complete design freedom is not possible, the transmission zeros constrain the regions of possible pole-zero placement. The effect of transmission zero constraints on the design possibilities, selection of transmission zeros and the avoidance of producing non-minimum phase transfer functions is the subject of the research being performed under this grant.

PROGRESS FOR 1 JULY - 1 SEPTEMBER 1992

EGR Activity

In the last progress report, it was proven that the determination of transmission zeros was a straightforward task using an expanded definition of Cramer's Rule or using Gauss' algorithm for determinants. It was also shown that the control law that decouples the system places poles at the transmission zero locations. In fact, the feedback recreates the eigenstructure of the decoupled subsystem associated with the transmission zeros, given by equ. 1 below:

$$\dot{x}_1(t) = [A_{11} - B_1 B_2^{-1} A_{21}] x_1(t) + A_{12} x_2(t) + B_1 u_c(t) \quad (1)$$

Because the transmission zeros $|s - A_{11} + B_1 B_2^{-1} A_{21}| = 0$ are invariant, the only way to reduce the excitation to $x_1(t)$, if it is desired to suppress the $x_1(t)$

response, is to try to decouple $x_1(t)$ from $x_2(t)$ and/or to interconnect the controllers in such a way that the effective control effectiveness B_1 is reduced, but this may not be desirable.

Transmission zeros are manifest only when fewer independent controllers than degrees of freedom of motion exist, and the primary purpose for decoupling is to provide for complete design freedom of the outputs $x_2(t)$ of the system, those motions of the airplane that we wish to control with exacting precision.

By decoupling, the design freedom of the output is complete and exacting, with many options open to the flight control system designer. The responses $x_2(t) = y(t)$ can be decoupled from each other or made to have any behavior desired. For instance, eigenvector assignment becomes a relatively straight-forward matrix algebra problem, and is shown to be a simple dynamic inversion approach to design. The objection to dynamic inversion (that the closed loop system is not robust) can also be easily overcome, at least in the system outputs $y(t) = x_2(t)$ and not just one, but an entire family of solutions is possible.

Consider the part of the system that was decoupled in such a way that the control effectiveness matrix B_2 is nonsingular, i.e., $|B_2| \neq 0$.

$$\dot{x}_2(t) = A_{22} x_2(t) + B_2 u(t) \quad (2)$$

Let us assume that we wish to design a system that behaves exactly as

$$\dot{y}(t) = Ly(t) + B_L u_c(t) \quad (3)$$

where the matrix L can be anything, including a Jordan form $L = \Lambda$ or a modified Jordan form L_m , i.e.

and solving for the control motion $u(t)$ will produce the required control law:

$$u(t) = B_2^{-1}[\dot{y}(t) + Px_2(t) - (A_{22} - P) y(t)] \quad (9)$$

An entire family of solutions can be obtained from equ. (9). For instance, by substituting for $\dot{y}(t)$ and choosing $A_{22} + P = L$, equ. (9) becomes

$$\begin{aligned} u(t) &= B_2^{-1}[Ly(t) + B_L u_c(t) + (L - A_{22}) x_2(t) - A_{22} y(t) - (L - A_{22}) y(t)] \\ &= B_2^{-1}[(L - A_{22}) x_2(t) + B_L u_c(t)] \end{aligned} \quad (10)$$

The substitution of the feedback control law of equ. (10) into equ. (2) yields

$$\begin{aligned} \dot{x}_2(t) &= A_{22}x_2(t) + B_2 B_2^{-1}[(L - A_{22}) x_2(t) + B_L u_c(t)] \\ &= L x_2(t) + B_L u_c(t) \end{aligned} \quad (11)$$

and the system behaves "exactly" as desired. If L was chosen non-interacting, the system would be decoupled. In block diagram form, the system is shown below. This architecture is often called "implicit model following."

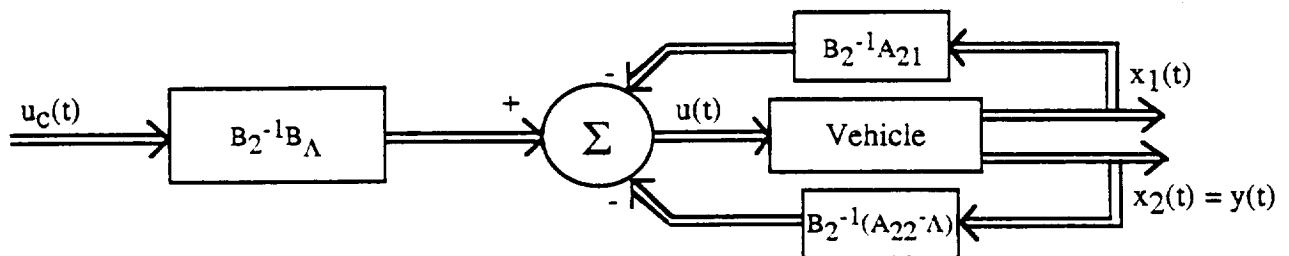


Fig. 1 Feedback Solution

The decoupling feedback $B_2^{-1}A_{21}$ has been added to the diagram to show the complete solution. If the plant contained as many independent controllers as degrees of freedom of motion (such as elevator/direct lift flap/throttle or elevator/thrust vectoring/throttle or even canard/thrust vectoring/throttle), the feedback $B_2^{-1}A_{21}x_1(t)$ would not be necessary, a complete dynamic inversion is possible. In general, if the matrix L of the system shown in fig. 1 has eigenvalues larger (i.e., farther in the lhp) than A_{22} , the robustness is improved from that of the open loop. The feedback is normally to augment the

aircraft natural dynamics in the "degenerative" rather than "regenerative" sense; stability is enhanced.

The same criteria, i.e., $\dot{y}(t) = Ly(t) + B_L u_c(t)$ can also be obtained without using feedback at all. All that is necessary is to calculate the forces and moments that must be applied to the aircraft to force it to behave as defined by equ. (11). This is done simply by defining $P = 0$ in equ. (9) above. Setting $P = 0$ in equation (9) yields the very simple solution

$$u(t) = B_2^{-1}[\dot{y}(t) - A_{22} y(t)] \quad (12)$$

indicating that $\dot{y}(t)$ and $y(t)$ are generated independently in a computer and the plant controllers are driven properly by the computer outputs $\dot{y}(t)$ and $y(t)$. The block diagram is shown in fig. 2 below. This architecture is often called "explicit model following."

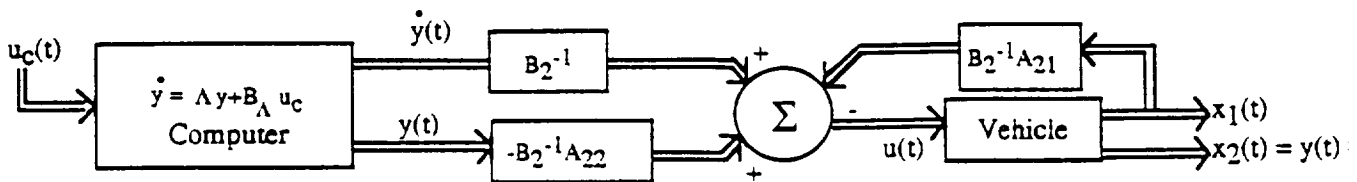


Fig. 2 Feedforward Solution

As indicated in equ. (12) and shown in fig. 2, the configuration is entirely an open loop architecture, yet yields "exactly" the same result as shown in fig. 1, a feedback solution. The control law "gains," B_2^{-1} and $B_2^{-1} A_{22}$ are a function only of the plant, and these gains constitute a complete dynamic inversion of the decoupled part of the plant. Because this is so, the model in the computer can be changed at will without changing the control law in any way. If, for instance, the flying qualities requirements were different for each flying task or flight regime, changing only the model dynamics will properly change the dynamic response. In fact, a ground-based simulator operates in exactly the way described above. The only difference is that the airplane is moving, not standing still, so the velocity and dynamic pressure dependent derivatives A_{22} are finite and must be taken into account.

The closed loop or feedback solution of fig. 1 and the open loop or "feedforward" solution of fig. 2 represent two extremes of the family of solutions that can be obtained. Neither system is particularly robust in the sense that flight condition variations of the stability and control derivatives B_2 and A_{22} will cause deviations in the desired response unless a lot of gain scheduling is used. Even with gain scheduling, the lack of low frequency robustness of the system shown in Fig. 2, would preclude its use in an actual airplane. However, robustness can be easily provided and in fact, the system shown in fig. 2, with feedback added, can result in a robust architecture, accounting for the variation of the stability and control derivatives of B_2 and A_{22} . In fact, there is reason to believe, as shown below, that minimal gain scheduling is possible for many aircraft.

The family of solutions that will yield a robust system configuration is given by the general solution of equ. (9). The block diagram of the system represented by equ. (9) (including the decoupling feedback) is shown in fig. 3 below:

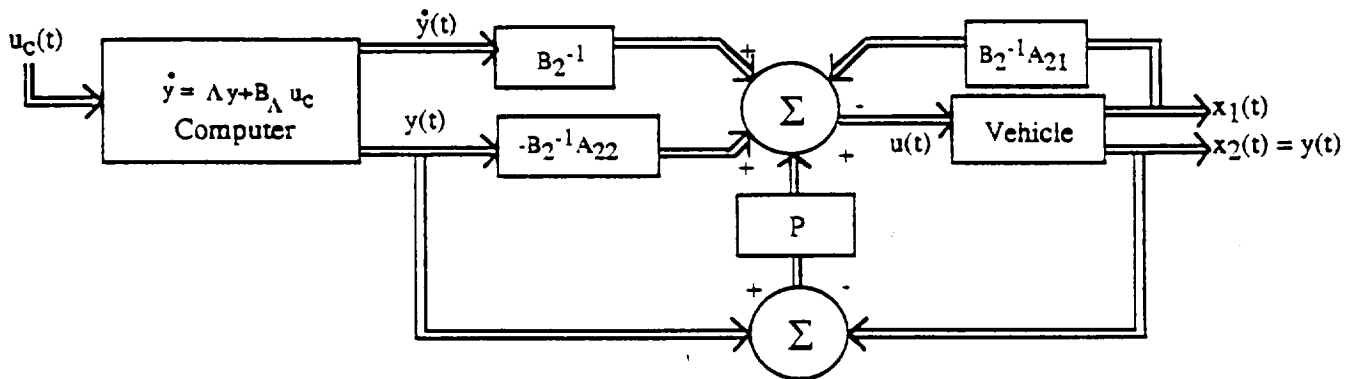


Fig. 3 General "Robust" Solution

The general solution of equ. (9), (i.e., fig. 3), shows that the matrix P acts on the error between the desired output $y(t)$ and the actual output $x_2(t)$. If B_2 and A_{22} are known "exactly", the error is zero and P has no function. In fact, P defines not only the regulation of the error between $y(t)$ and $x_2(t)$ but also defines the perturbation response of $x_2(t)$ to external disturbances (gust alleviation). Most importantly, because P can be an integration process, low frequency robustness can be provided, so the response of the computer output and the aircraft output will not diverge. Because all the flying qualities requirements can be resident in the computer model, the gust alleviation or

structural mode control function can be done using feedback without affecting the maneuvering flying qualities requirements. In fact, equ. 9 is simply a formalization of the present common practice of providing feed forward gains in a flight control design.

If the computer is programmed such that the kinematics of the plant are resident in the computer but the aerodynamics in the computer are chosen for flying qualities purposes, the computer can represent a global "model following" system. If such a system were used for a wide flight range vehicle such as HSCT, the HSCT vehicle would always be at the same flight condition as the computer generated "model," but the HSCT vehicle would respond dynamically as the "level 1" flying qualities model. There is reason to believe that the configuration defined by fig. 3 would work well for a wide flight range vehicle.

Because the function P acts on the error between the computer generated model response and the actual vehicle response, P can represent a robust compensator as defined by such methods as an H_∞ system designed to minimize the error as the stability and control derivatives A_{22} and B_2 vary with flight condition.

In general, any compensation network can be expanded in partial fraction expansion form to represent proportional, integral and derivative components (or designed as a PID system). To show how such a network could be designed for an architecture of this type, consider a PID system, resulting in an error control law.

$$u_e(t) = -K_1 e(t) - K_2 \int e(t) dt - K_3 \dot{e}(t) \quad (13)$$

shown in fig. 4 below:

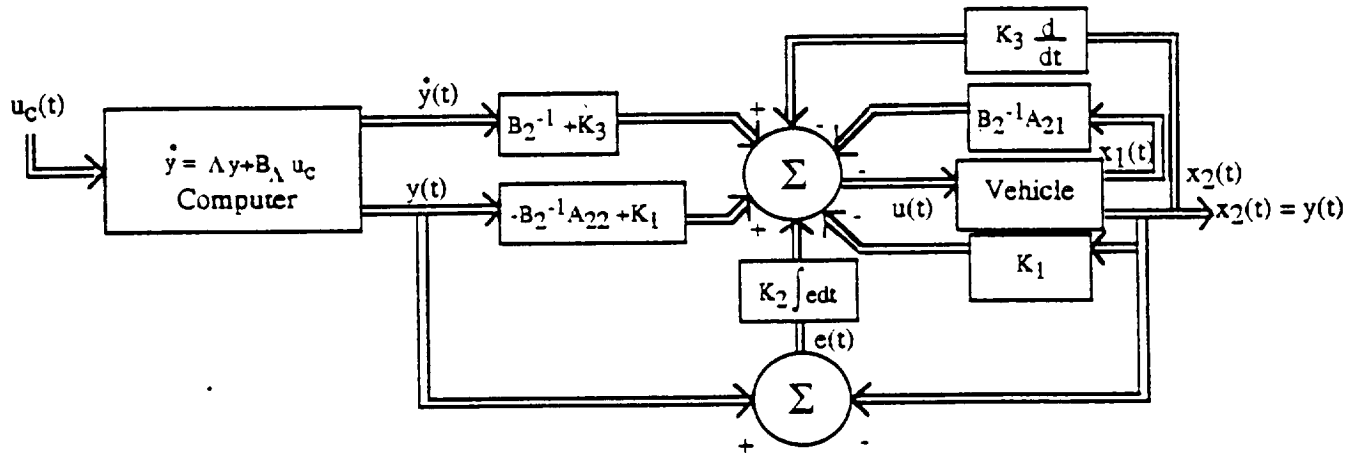


Fig. 4 More Specific "Robust" Solution

This block diagram is drawn to highlight the effects of the PID feedback and the effect of this feedback on the response of the system as stability and control derivatives B_2 and A_{22} vary in flight. As shown in the figure, the accuracy of the design depends upon the accuracy of B_2 and A_{22} , the matrices involved in the dynamic inversion. If the feedback gains are made sufficiently large, the system can be made insensitive to variations in the stability and control derivatives, i.e.,

- if $K_3 \gg B_2^{-1}$ → insensitive to variations in control effectiveness and in control surface nonlinearities
- if $K_1 \gg -B_2^{-1} A_{22}$ → insensitive to variations in $B_2^{-1} A_{22}$, i.e., the stability derivatives

Making the fair assumption that the feedback is to maintain or improve the stability of the vehicle, the integral of the error will guarantee $x_2(t) = y(t)$ in the long term, regulating always about the trajectory of the airplane on the model computer (for instance, a hypersonic NASP with ideal level 1 flying qualities) without the need to directly measure some air data (such as velocity) on the vehicle itself. Because the integral guarantees long term zero error, the pilot command input-response output is independent of flight condition and can be made constant or vary with flight condition exactly as specified (F_s vs. n_z) in the F.Q. specifications. Because in the long term the aircraft steady state

response will be totally predictable, a display of the pilot command input will tell the pilot what the steady state flight variable changes will be regardless of the sluggishness of the vehicle response, resulting in a "predictor" display. By limiting commands at the model, functions such as angle of attack and sideslip can be limited, again useful for a NASP system. The problem solving potential of this type of system architecture seems significant.

Even more advantages for this architecture can be realized. For instance, because the gains $B_2^{-1} A_{22}$ represent a "division" process of dimensional stability and control derivatives, many of which are dimensionalized in exactly the same way, many of the terms of $B_2^{-1} A_{22}$ are simply (constant) ratios of non-dimensional stability derivatives, such as $c_{m\alpha}/c_{m\delta_e}$, which can be accurately obtained in a wind tunnel. These constants occur along the diagonal of the matrix $B_2^{-1} A_{22}$, so the robustness oriented gains would be designed to minimize the effects of off-diagonal terms, (if their effect is significant). Because the aircraft can be made to respond to disturbances entirely independently of the computer model (which doesn't respond at all unless turbulence is measured and injected into the computer), the feedback can be tailored for gust alleviation or structural mode control or even to minimize wing root bending moments (to disturbances) without affecting flying qualities (resident in the computer). The minimization of maneuver loads can be dealt with in the model computer and reflected in the vehicle itself. For instance, if the "model" had a direct lift flap, distribution of "model" wing loads would be reflected in the vehicle itself.

To the designer, perhaps the biggest advantage is the fact that most of the ground based simulator setup can be transferred to the actual vehicle, accounting only for the fact that the actual airplane is moving rather than standing still. Accurate evaluation of the differences in pilot opinion between the ground based simulator and the actual vehicle can be made. In a simulator, the velocity is displayed to the pilot; in the actual airplane, not only can the velocity from the computer model be displayed, but the airplane will be moving that fast.

It is clear that the sensitive part of the type of system described herein is $x_1(t)$, the dynamics decoupled from $x_2(t)$. This will be particularly true if the

transmission zeros are relatively low frequency. Because the "outputs" and measurement set or sensors can be entirely different, it may be possible, using observer synthesis ideas of Bacon (Langley) to improve the robustness of the $u(t) = -B_2^{-1} A_{21} x_1(t)$ feedback portion of the system. These possibilities will be considered by EGR during the next reporting period.

Flying Qualities Implications

It is not to suggest that decoupling will solve all flying qualities problems. The consequences of decoupling can be considerable. Consider the relatively simple modal decoupling design approach used in the Shuttle, which used pitch rate feedback and proportional plus integral compensation in the error loop. This pitch rate pole-zero canceling scheme essentially eliminated a phugoid mode residue in pitch rate, but increased the phugoid contribution to the $\alpha(t)$ response. The closed loop $\alpha(t)$ transfer function contains a pole at the origin, and a step stick command will yield a smooth, well-behaved pitch rate response, but the angle of attack will be divergent. Since $\gamma = \theta - \alpha$, the attitude and flight path will not be harmony, i.e., the vehicle flight path will wander if the pilot holds a steady attitude. A pilot wants flight path proportional to attitude, so this kind of system may produce a PIO problem for the pilot, particularly during flare and landing.

As the astronaut pilot pulls (or if he has learned correctly, pulsed) the stick to flare to a new pitch angle, the lift ($-Z_\alpha \alpha$) increases because $\alpha(t)$ is divergently increasing, and the vehicle will have a tendency to "float" down the runway. The increase in $\alpha(t)$ increases induced drag, decreasing the velocity and decreasing Z_α . So eventually either the vehicle will settle to the runway (decreasing Z_α greater affect than increasing α) or the vehicle will stall. The pilot may have to pulse forward on the stick to get down. Pilots do not like to push on the stick to settle on the runway, they usually depend on the phugoid response to settle the airplane down, (but nonexistent in a rate command, attitude hold system). Also, since $\frac{\Delta \dot{\gamma}}{\Delta q} \doteq \frac{1/T_{\theta 2}}{s + 1/T_{\theta 2}}$, the pilot must cope with the delay or time constant (2-2.5 sec in the Shuttle) of the flight path bending response after initiating a pitch rate response; the astronaut pilot must develop a considerable precognitive predictive capability. When coupled with the

elevon location on the Shuttle, which suggests that the pilot sits aft of the center of rotation (percussion), thereby producing an initial "wrong direction cue" or time delay, then the Shuttle PIO evident in an early Shuttle flight is no surprise; accuracy or "tight" flight path control is out of the question. The extensive (and expensive) astronaut-pilot training is justified. It would appear that a little static stability (i.e., $\alpha(t)$ feedback) would help the Shuttle settle to the runway and provide for a better capability to maneuver near the ground without a PIO tendency.

The result is that decoupling can significantly alter the eigenvector configuration of the vehicle, and change response residues in such a way that the vehicle no longer behaves in an "airplane-like" fashion. If the kind of change in vehicle behavior can be produced in a relatively simple decoupling situation as evidenced on the Shuttle, then multivariable decoupling may be expected to complicate the flying qualities scenario even more. Decoupling may be a blessing or a curse, and much research must yet be done to define the blessings and the curses.

Generally speaking, it is an objective of "reconfiguration" technology to switch to an alternate set of control effectors upon the failure of a control surface, without changing the dynamic response of the vehicle. If the original decoupling was obtained using primary control effectors (i.e., elevator \rightarrow pitching moment, direct left flap \rightarrow lift or flight path, and/or throttle \rightarrow velocity) the likelihood that the transmission zeros will be rhp is small. If a switch is made to a secondary set of controllers during reconfiguration to maintain the same non-interaction, the likelihood of rhp transmission zeros is considerably increased. It might be prudent to abandon the decoupling criteria during reconfiguration and revert to a flying qualities criteria that would result in a "conventionally flying airplane."

Examples of the changes in transmission zeros as a function of controller sets to achieve the same decoupled behavior will be shown in the next reporting period.

CUBRC Contract 1730
NASA Contract NAG-1-1361
University at Buffalo Progress Report: 7/1/92-9/1/92

The theoretical developments and underpinning of the transmission zero work are described in the section titled "EGR activity." The U.B. activity includes and/or is based on this theory, but for brevity the reporting of these developments is not repeated here.

The major activity of the reporting period was the creation, debugging, and transfer (to EGR) of detailed computer simulations to be used for testing and demonstrating the theoretical developments. The computer simulations represent the experimental Total In Flight Simulator (TIFS) aircraft, operated by the CALSPAN Flight Research Department.

For simulation purposes, the TIFS is assumed to be flying as a rigid body in a vertical (longitudinal) plane, so that there are three degrees-of-freedom (horizontal translation x , vertical translation z , and pitch angle θ). Aerodynamic coefficients are consistent with Calspan reports. The details of the simulation follow.

Coordinate Systems

In developing the aircraft equations of motion, two different coordinate systems are used, shown in Figure 1. One is an inertial coordinate system, which is fixed to the earth and is considered to be a non-rotating system. This is a valid assumption since the rotation of the earth is negligible in most aircraft dynamic problems. The other system is fixed to the aircraft center of gravity and rotates along with the aircraft. This system is referred to as the body axis coordinate system.

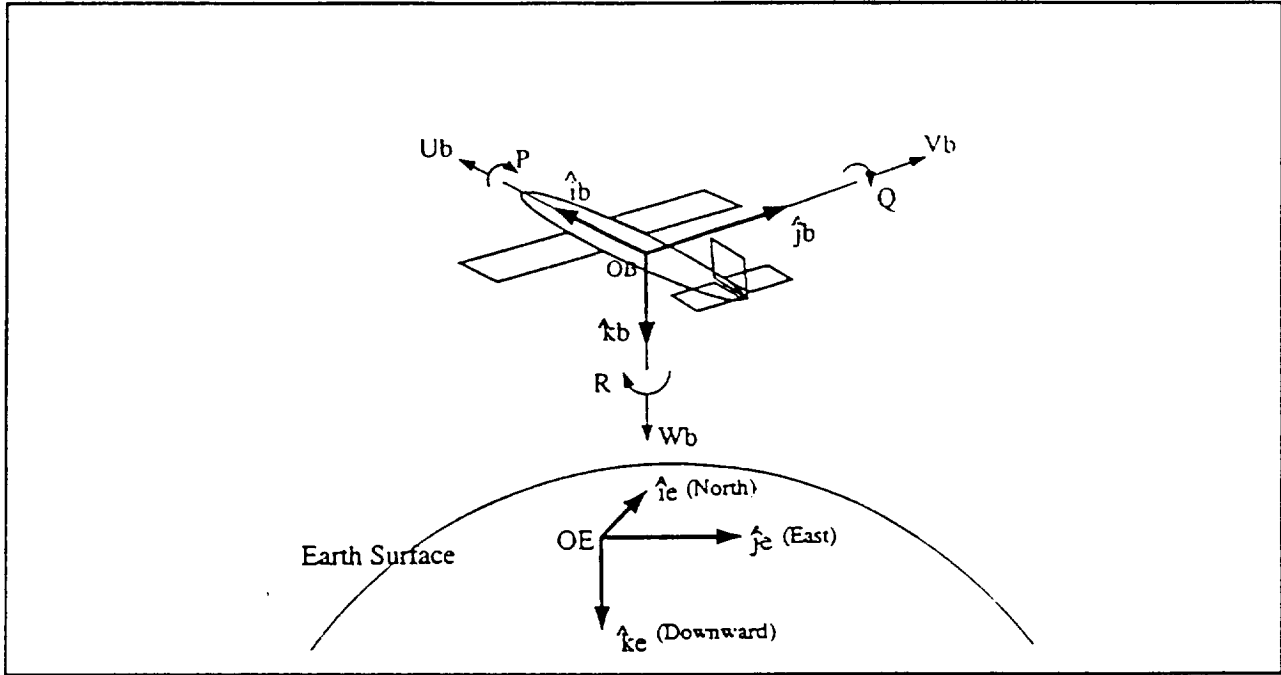


Figure 1 Coordinate Axis System

Equations of Motion

Newton's second law is used to derive the rigid body equations of motion, i.e., the conservation of both linear and angular momentum (Nelson [2]):

$$\sum \vec{F} = \frac{d}{dt} \sum (m\vec{v}) \quad (1)$$

$$\sum \vec{M} = \frac{d}{dt} \vec{H} = \frac{d}{dt} \sum \vec{r} \times m\vec{v} \quad (2)$$

The airplane is considered as a continuum of mass particles (δm) and each elemental mass has a velocity (\vec{v}) relative to an inertial frame. Newton's second law is:

$$\delta \vec{F} = \delta m \frac{d\vec{v}}{dt} \quad (3)$$

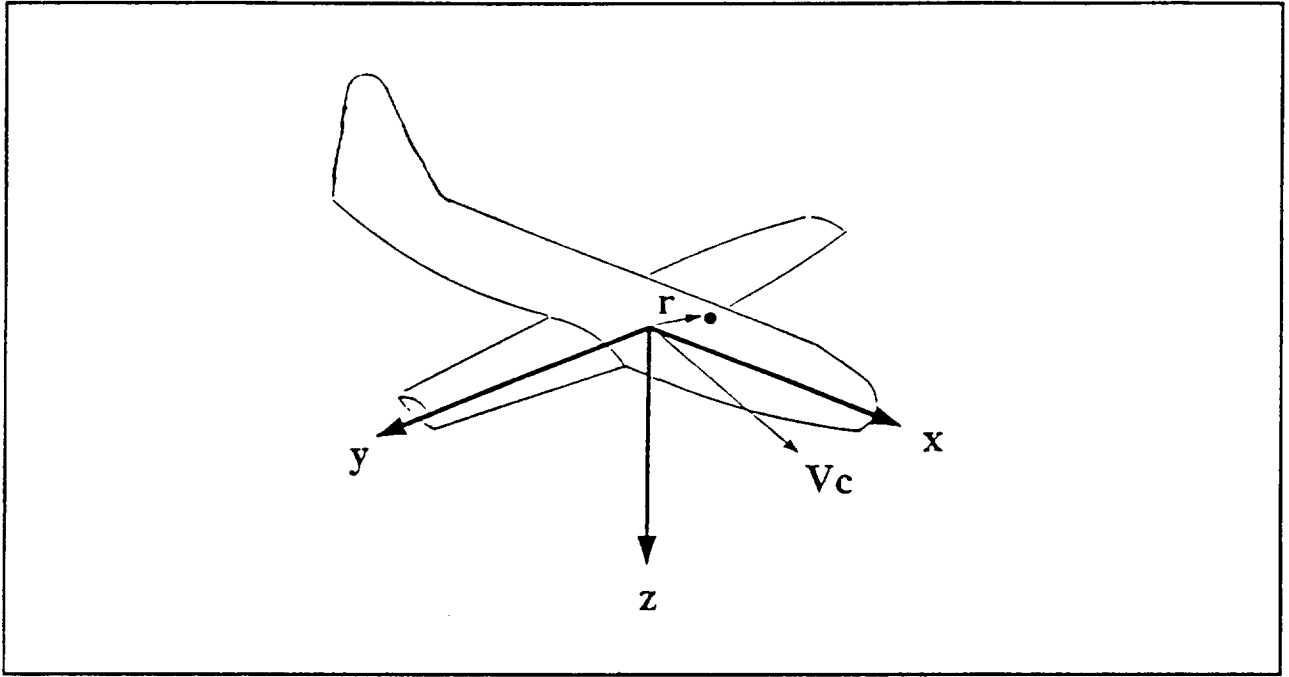


Figure 2 Body Axis System

From Figure 2, the velocity of the differential mass can be expressed as:

$$\vec{v} = \vec{v}_c + \frac{d\vec{r}}{dt} \quad (4)$$

Since the mass of the aircraft is assumed constant and the total mass of the aircraft is found by summing the mass elements, Newton's second law may be written as:

$$\sum \delta \vec{F} = \vec{F} = m \frac{d\vec{v}}{dt} + \frac{d^2}{dt^2} \sum (\vec{r}) \delta m \quad (5)$$

The right hand side of Equation (5) equals zero since \vec{r} is taken from the center of mass. Equation (5) now reduces to:

$$\vec{F} = m \frac{d\vec{v}_c}{dt} \quad (6)$$

The moment equation is developed in terms of the relative velocity of a mass element to the center of mass:

$$\vec{v} = \vec{v}_c + \frac{d\vec{r}}{dt} = \vec{v}_c + \vec{\omega} \times \vec{r} \quad (7)$$

where $\vec{\omega}$ is the angular velocity of the aircraft. Substituting this expression into the moment Equation (2), the total moment of momentum is:

$$\vec{H} = \sum (\vec{r})\delta m \times \vec{v}_c + \sum [\vec{r} \times (\vec{\omega} \times \vec{r})]\delta m \quad (8)$$

Again, the left hand side of Equation (8) equals zero and the moment of momentum equation reduces to:

$$\vec{H} = \sum [\vec{r} \times (\vec{\omega} \times \vec{r})]\delta m \quad (9)$$

A difficulty occurs if the reference is rotating, since the moment will vary with time. To eliminate this difficulty, a transformation of the reference frame is made to the body axis system (onto the aircraft). A vector \vec{A} is transformed from a fixed system to a rotating coordinate system by:

$$\left. \frac{d\vec{A}}{dt} \right|_{fixed} = \left. \frac{d\vec{A}}{dt} \right|_{rot.} + [\vec{\omega} \times \vec{A}] \quad (10)$$

The force and moment equations, transformed into the body axis system, now become:

$$\vec{F} = m \frac{d\vec{v}_c}{dt} + m(\vec{\omega} \times \vec{v}_c) \quad (11)$$

$$\vec{M} = \frac{d\vec{H}}{dt} + (\vec{\omega} \times \vec{H}) \quad (12)$$

Vector Components and Scalar Equations

To obtain the time history results of Equations (11) and (12), it is necessary to express the vector equations into component form. The component forms of the forces, moments, gravity, linear and angular velocities are shown in Figure 3.¹ The corresponding equations are:

$$\begin{aligned} \vec{F} &= F_x \vec{i} + F_y \vec{j} + F_z \vec{k} \\ \vec{M} &= L \vec{i} + M \vec{j} + N \vec{k} \\ \vec{g} &= g_x \vec{i} + g_y \vec{j} + g_z \vec{k} \\ \vec{\omega} &= P \vec{i} + Q \vec{j} + R \vec{k} \\ \vec{V}_p &= U \vec{i} + V \vec{j} + W \vec{k} \\ \vec{r} &= x \vec{i} + y \vec{j} + z \vec{k} \end{aligned} \quad (13)$$

¹ Positive sense is in the direction of the arrows

Equation (11) can now be expanded into scalar form:

$$\begin{aligned}
 F_x + mg_x &= m(\dot{U} - VR + WQ) \\
 F_y + mg_y &= m(\dot{V} + UR - WP) \\
 F_z + mg_z &= m(\dot{W} - UQ + VP)
 \end{aligned}
 \tag{14}$$

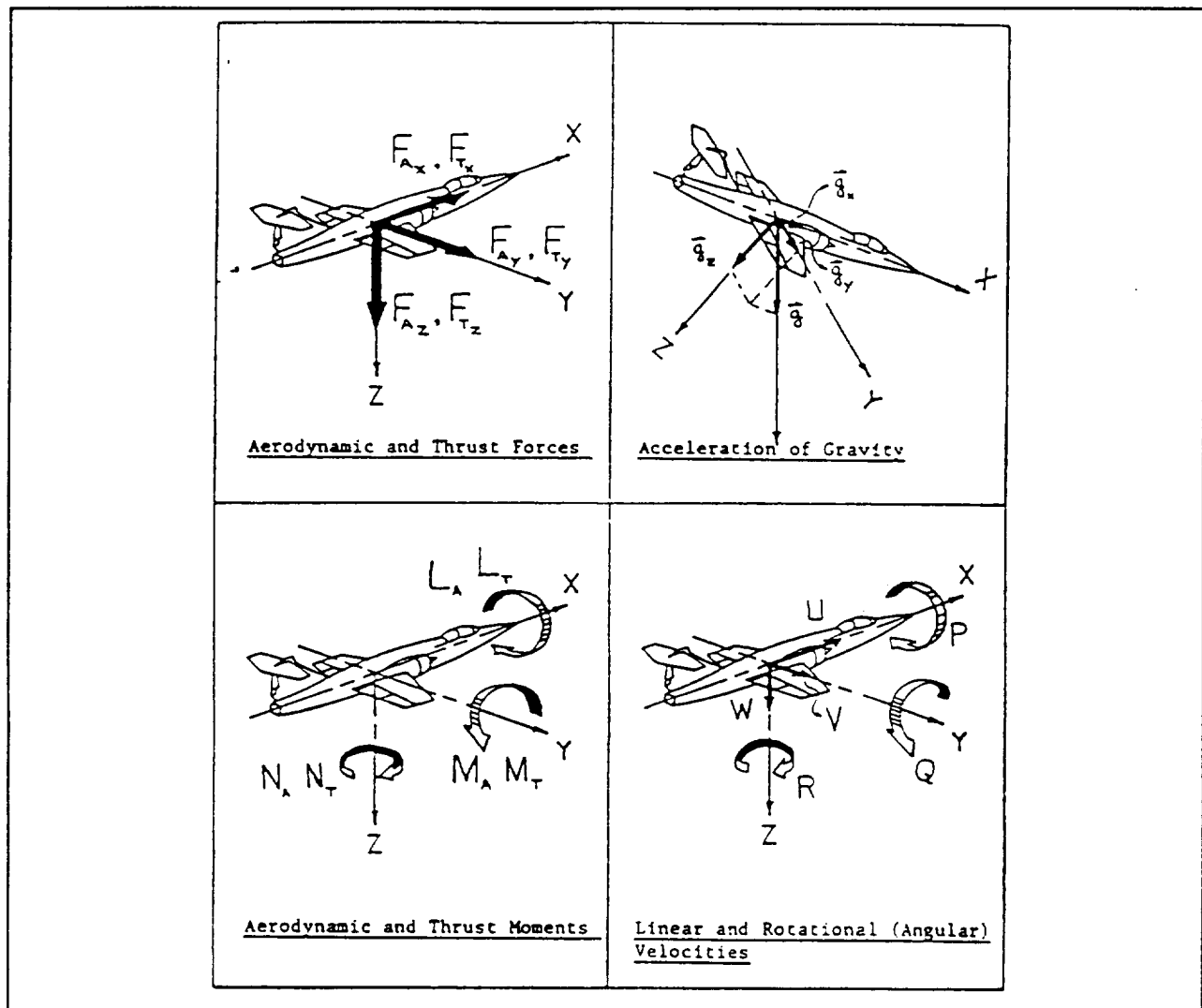


Figure 3 Vector Components (from Roskam [1])

After expanding Equation (9), the scalar components of the moment of momentum are:

$$\begin{aligned}
H_x &= P \sum (y^2 + z^2) \delta m - Q \sum (xy) \delta m - R \sum (xz) \delta m \\
H_y &= -P \sum (xy) \delta m + Q \sum (x^2 + z^2) \delta m - R \sum (yz) \delta m \\
H_z &= -P \sum (xz) \delta m - Q \sum (yz) \delta m + R \sum (x^2 + y^2) \delta m
\end{aligned} \tag{15}$$

These equations can be expressed in terms of mass moments of inertia about the x, y, and z axes:

$$\begin{aligned}
H_x &= I_{xx}P - I_{xy}Q - I_{xz}R \\
H_y &= -I_{xy}P + I_{yy}Q - I_{yz}R \\
H_z &= -I_{xz}P - I_{yz}Q + I_{zz}R
\end{aligned} \tag{16}$$

Since, for most airplanes, the X-Z plane is a plane of symmetry, the moments of inertia for $I_{xy} = I_{yz} = \text{zero}$. With this assumption, and applying Equations (16) to the moment expression in Equation (12), the scalar moment equations can be written as:

$$\begin{aligned}
L &= I_{xx}\dot{P} - I_{zz}\dot{R} - I_{xz}PQ + (I_{zz} - I_{yy})RQ \\
M &= I_{yy}\dot{Q} + (I_{xx} - I_{zz})PR + I_{zz}(P^2 - R^2) \\
N &= I_{zz}\dot{R} - I_{xx}\dot{P} + (I_{yy} - I_{xx})PQ + I_{zz}QR
\end{aligned} \tag{17}$$

where L , M and N are the moments about the X, Y and Z axes, respectively.

Earth Fixed System and the Kinematic Equations

The force and moment equations are derived in the body-fixed axis system. But, the position of the aircraft must be described by the earth-fixed coordinate system. This is accomplished by three *consecutive* rotations (whose order is important). From Figure 4, the following rotations are made:

1. Rotate the $X_1Y_1Z_1$ body coordinate frame about the Z_1 axis over the **yaw** angle (Ψ) to the $X_2Y_2Z_2$ body coordinate frame.
2. Rotate the $X_2Y_2Z_2$ body coordinate frame about the Y_2 axis over the **pitch** angle (Θ) to the $X_3Y_3Z_3$ body coordinate frame.
3. Rotate the $X_3Y_3Z_3$ body coordinate frame about the X_3 axis over the **roll** angle (Φ) to the XYZ inertial coordinate frame.

These angles (yaw, pitch and roll) are known as the *Euler* angles.

The velocity components between the body-fixed coordinate system and the earth-fixed coordinate system are related by a set of orthogonal transformations (a more complete derivation may be found in [1] and [2]). These transformations are:

$$\begin{Bmatrix} \dot{x} \\ \dot{y} \\ \dot{z} \end{Bmatrix} = \begin{Bmatrix} C_\Theta C_\Psi & S_\Phi S_\Theta C_\Psi - C_\Phi S_\Psi & C_\Phi S_\Theta C_\Psi + S_\Phi S_\Psi \\ C_\Theta S_\Psi & S_\Phi S_\Theta S_\Psi + C_\Phi C_\Psi & C_\Phi S_\Theta S_\Psi - S_\Phi C_\Psi \\ -S_\Theta & S_\Phi C_\Theta & C_\Phi C_\Theta \end{Bmatrix} \begin{Bmatrix} U \\ V \\ W \end{Bmatrix} \quad (18)$$

where $C_\Phi \equiv \cos(\Phi)$, $S_\Psi \equiv \sin(\Psi)$, etc.

The kinematic equations relate the Euler angles (Ψ , Θ and Φ) and the angular velocities (P, Q and R). From Figure 4, $\vec{\omega}$ must equal the vector sum of the time rate of change of the Euler angles about the \vec{k}_1 , \vec{j}_2 , and \vec{i}_3 axes:

$$\vec{\omega} = \dot{\Psi} \vec{k}_2 + \dot{\Theta} \vec{j}_3 + \dot{\Phi} \vec{i} \quad (19)$$

Using transformations similar to Equation (18) and from Equation (13), the angular velocity may be written as:

$$\begin{aligned} \vec{\omega} = P\vec{i} + Q\vec{j} + R\vec{k} = \vec{i}(-\dot{\Psi} \sin \Theta + \dot{\Phi}) + \\ \vec{j}(\dot{\Psi} \cos \Theta \sin \Phi + \dot{\Theta} \cos \Phi) \\ \vec{k}(\dot{\Psi} \cos \Theta \cos \Phi - \dot{\Theta} \sin \Phi) \end{aligned} \quad (20)$$

Equating components, the kinematic equations become (in matrix form):

$$\begin{Bmatrix} P \\ Q \\ R \end{Bmatrix} = \begin{Bmatrix} 1 & 0 & -\sin \Theta \\ 0 & \cos \Phi & \cos \Theta \sin \Phi \\ 0 & -\sin \Phi & \cos \Theta \cos \Phi \end{Bmatrix} \begin{Bmatrix} \dot{\Phi} \\ \dot{\Theta} \\ \dot{\Psi} \end{Bmatrix} \quad (21)$$

The time histories of the Euler angles are determined by inverting the 3x3 matrix in Equation (21):

$$\begin{aligned} \dot{\Phi} &= P + Q \sin \Phi \tan \Theta + R \cos \Phi \tan \Theta \\ \dot{\Theta} &= Q \cos \Phi - R \sin \Phi \\ \dot{\Psi} &= (Q \sin \Phi + R \cos \Phi) \sec \Theta \end{aligned} \quad (22)$$

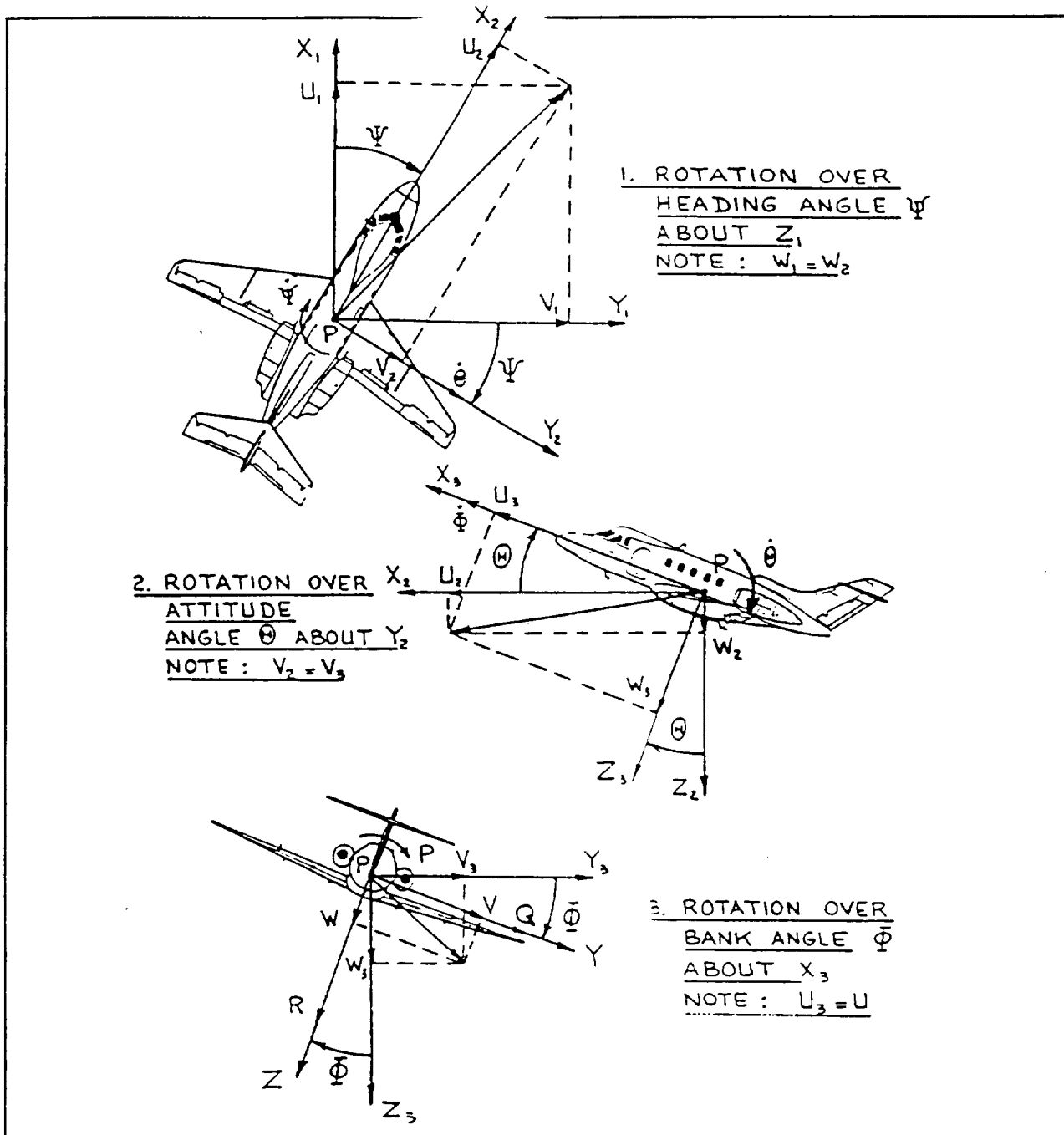


Figure 4 Rotation from Earth-Fixed to Body-Fixed Frame (from Roskam [1])

Aerodynamic Nomenclature

All forces and moments developed are based on the stability axes system defined by Figure 5. This system is utilized since experimental data from wind tunnel tests are presented in the stability axes. The stability axes are obtained by rotating the body axes (XYZ) about the $Y = Y_s$,

axis. This is done over a rotational angle α (known as the angle of attack) until the body-fixed axis (X-axis) coincides with the free stream velocity vector (\vec{V}_{p1}).

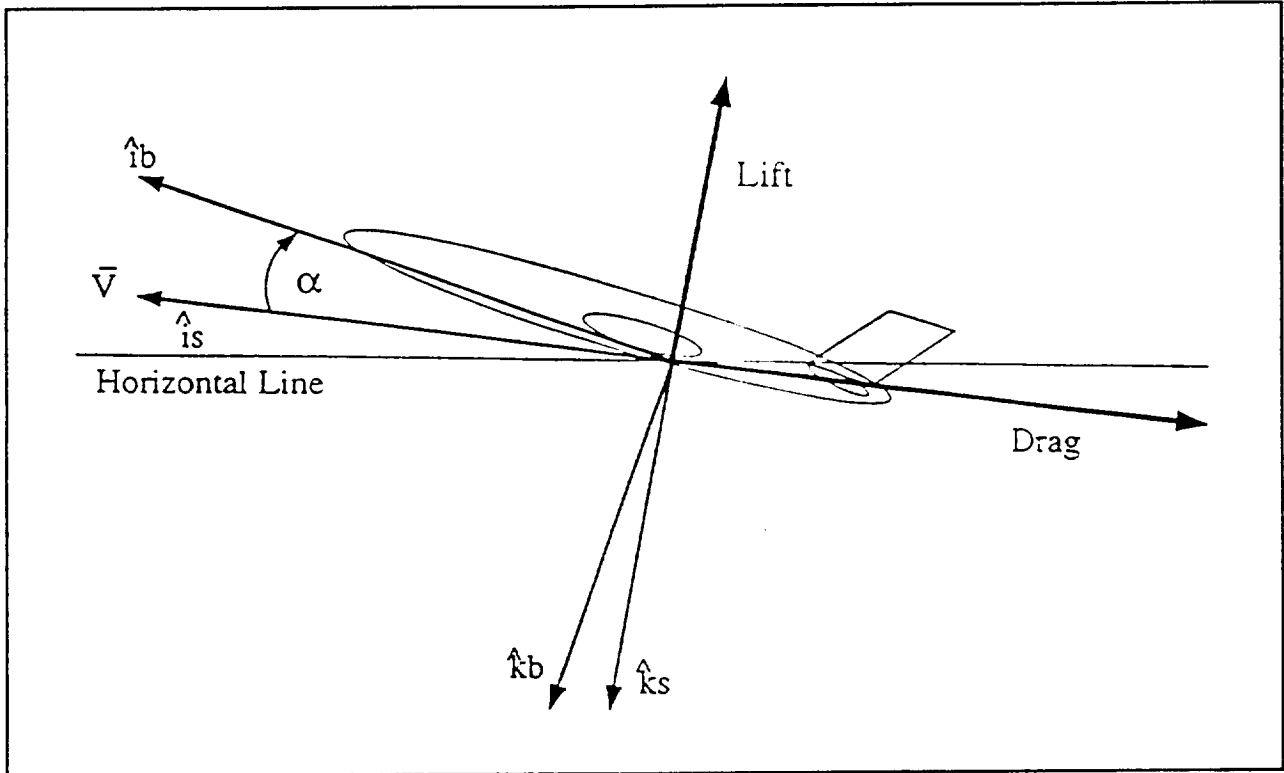


Figure 5 Stability Axis

The equation for the angle of attack is:

$$\alpha = \tan^{-1} \frac{W}{U} \quad (23)$$

The equation for the airspeed is:

$$V_p = \sqrt{(U^2 + V^2 + W^2)} \quad (24)$$

The flight path angle (γ) is the difference between the pitch angle and the angle of attack ($\gamma = \Theta - \alpha$). Figure 6 depicts the relationship between the different coordinate axes in the longitudinal plane.

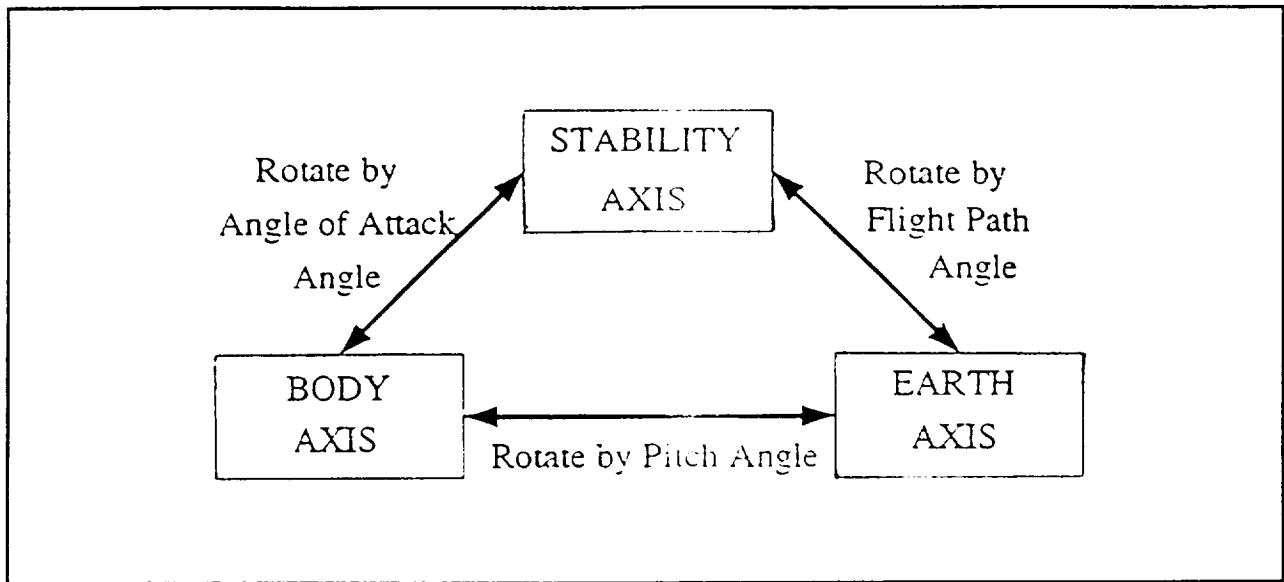


Figure 6 Relationship Between the Earth, Body and Stability Axis Frame

Forces and Moments

To simplify the analysis, all forces and moments are developed in the stability axis system. The force (\vec{F}^s) and moment (\vec{M}^s) components are:

$$\begin{aligned}\vec{F}^s &= F_{A_x}^s \vec{i}_s + F_{A_y}^s \vec{j}_s + F_{A_z}^s \vec{k}_s = -D \vec{i}_s + F_Y \vec{j}_s - L \vec{k}_s \\ \vec{M}^s &= L_A \vec{i}_s + M_A \vec{j}_s + N_A \vec{k}_s\end{aligned}\quad (25)$$

where D = Drag, L = Lift and F_Y = Sideforce. L_A , M_A and N_A are aerodynamic moments.

The steady state forces and moments for a straight line flight are assumed to depend only on angle of attack (α), sideslip angle (β), thrust and the control surface deflections of the elevator (δ_E), ailerons (δ_A), rudder (δ_R), and aerodynamic coefficients. These dimensionless coefficients are comprised of derivatives evaluated at constant Mach and Reynolds number (e.g.):

$$C_D = C_{D_0} + C_{D_\alpha} \alpha + C_{D_{\delta_E}} \delta_E \quad (26)$$

where:

- C_{D_0} = total airplane drag coefficient for $\alpha = \delta_E = 0$.
- C_{D_α} = total airplane drag change with angle of attack for $\delta_E = 0$.
- $C_{D_{\delta_E}}$ = total airplane drag change with elevator angle for $\alpha = 0$.

A similar analysis is made for the remaining aerodynamic coefficients.

The aerodynamic forces and moments are expressed in terms of the dimensionless coefficients, flight dynamic pressure, characteristic length (for the moments only) and a reference area:

$$\begin{aligned} D &= C_D \bar{q} S = (C_{D_0} + C_{D_\alpha} \alpha + C_{D_{\delta_E}} \delta_E) \bar{q} S \\ F_Y &= C_{F_Y} \bar{q} S = (C_{Y_\beta} \beta + C_{Y_{\delta_A}} \delta_A + C_{Y_{\delta_R}} \delta_R) \bar{q} S \\ L &= C_L \bar{q} S = (C_{L_0} + C_{L_\alpha} \alpha + C_{L_{\delta_E}} \delta_E) \bar{q} S \end{aligned} \quad (27)$$

$$\begin{aligned} L_A &= C_l \bar{q} S b \\ &= \left(C_{l_\beta} \beta + C_{l_{\delta_A}} \delta_A + C_{l_{\delta_R}} \delta_R + C_{l_P} \frac{Pb}{2U_s} + C_{l_R} \frac{Rb}{2U_s} \right) \bar{q} S b \\ M_A &= C_M \bar{q} S \bar{c} \\ &= \left(C_{M_0} + C_{M_\alpha} \alpha + C_{M_{\delta_E}} \delta_E + C_{M_Q} \frac{Q\bar{c}}{2U_s} \right) \bar{q} S \bar{c} \\ N_A &= C_N \bar{q} S b \\ &= \left(C_{N_\beta} \beta + C_{N_{\delta_A}} \delta_A + C_{N_{\delta_R}} \delta_R + C_{N_P} \frac{Pb}{2U_s} + C_{N_R} \frac{Rb}{2U_s} \right) \bar{q} S b \end{aligned} \quad (28)$$

The flight dynamic pressure is :

$$\bar{q} = \frac{1}{2} \rho U_s^2 \quad (29)$$

where ρ is the air density and U_s is the aircraft's airspeed.

The aircraft thrust vector is also divided into components:

$$\begin{aligned} F_{T_x}^s &= T \cos(\alpha) \\ F_{T_y}^s &= 0 \\ F_{T_z}^s &= -T \sin(\alpha) \\ L_T^s &= 0 \\ M_T^s &= -T d_T \\ N_T^s &= 0 \end{aligned} \quad (30)$$

where d_T is the moment arm of thrustline.

For a *trimmed* airplane, the forces and moments acting on it are in equilibrium. This is accomplished when the pitching moment equals zero and when the lift equals the airplane

weight. Using Equations (27) and (28):

$$\begin{aligned} 0 &= \left(C_{M_0} + C_{M_\alpha} \alpha + C_{M_{\delta_E}} \delta_E \right) \\ \frac{mg}{\bar{q}S} = C_{L_{trim}} &= \left(C_{L_0} + C_{L_\alpha} \alpha + C_{L_{\delta_E}} \delta_E \right) \end{aligned} \quad (31)$$

Solving these equations for α and δ_E determines the trim value for the angle of attack and the trim elevator setting:

$$\alpha_{trim} = \frac{C_{L_{trim}} C_{M_{\delta_E}} - C_{L_0} C_{M_{\delta_E}} + C_{L_{\delta_E}} C_{M_0}}{C_{L_\alpha} C_{M_{\delta_E}} - C_{L_{\delta_E}} C_{M_\alpha}} \quad (32)$$

$$\delta_{E_{trim}} = \frac{C_{L_{trim}} C_{M_\alpha} - C_{L_0} C_{M_\alpha} + C_{L_\alpha} C_{M_0}}{C_{L_{\delta_E}} C_{M_\alpha} - C_{L_\alpha} C_{M_{\delta_E}}} \quad (33)$$

Combining the rigid body equations and the aircraft kinematic equations yields a full set of flight dynamics equations that describe any aircraft flight path or motion. To accomplish this, all forces must first be transformed from the stability axis system to the body axis system. From Figure 5:

$$\begin{aligned} F_z^b &= -D \cos(\alpha) + L \sin(\alpha) + T \cos(\alpha) \\ F_y^b &= F_y^s \\ F_x^b &= -D \sin(\alpha) - L \cos(\alpha) + T \sin(\alpha) \end{aligned} \quad (34)$$

The force equations (14) are then solved in terms of the linear velocity rates (\dot{U} , \dot{V} and \dot{W}). Also, the moment equations (17) are solved in terms of the angular velocity rates (\dot{P} , \dot{Q} and \dot{R}). To simplify the analysis, let:

$$\begin{aligned} k_1 &= I_{XZ}(I_{YY} - I_{XX}) \\ k_2 &= I_{ZZ}(I_{ZZ} - I_{YY}) \\ k_3 &= I_{XZ}(I_{ZZ} - I_{YY}) \\ k_4 &= I_{XX}(I_{YY} - I_{XX}) \end{aligned} \quad (35)$$

The full flight dynamic motions are now expressed as a 12th order set of nonlinear differential equations (three of which are simple integrations of the linear velocities to yield linear positions). These equations can now be integrated to yield flight trajectories, after a transformation is made

to the earth-fixed coordinate system by Equation (18), of any variable (e.g. plane altitude, airspeed, etc).

$$\dot{U} = -g \sin(\Theta) + \frac{F_x^b}{m} + VR - WQ \quad (36)$$

$$\dot{V} = g \sin(\Phi) \cos(\Theta) + \frac{F_y^b}{m} - UR + WP \quad (37)$$

$$\dot{W} = g \cos(\Phi) \cos(\Theta) + \frac{F_z^b}{m} + UQ - VP \quad (38)$$

$$\dot{P} = \frac{I_{XZ}N_A + I_{ZZ}L_A - k_1PQ - I_{XZ}^2QR + I_{XZ}I_{ZZ}PQ - k_2RQ}{I_{XX}I_{ZZ} - I_{XZ}^2} \quad (39)$$

$$\dot{Q} = \frac{M_A - (I_{XX} - I_{ZZ})PQ - I_{XZ}(P^2 - R^2)}{I_{YY}} \quad (40)$$

$$\dot{R} = \frac{I_{XX}N_A + I_{XZ}L_A + I_{XZ}^2PQ - k_3RQ - k_4PQ - I_{XX}I_{XZ}QR}{I_{ZZ}I_{XX} - I_{XZ}^2} \quad (41)$$

$$\dot{\Theta} = Q \cos \Phi - R \sin \Phi \quad (42)$$

$$\dot{\Psi} = (Q \sin \Phi + R \cos \Phi) \sec \Theta \quad (43)$$

$$\dot{\Phi} = P + Q \sin \Phi \tan \Theta + R \cos \Phi \tan \Theta \quad (44)$$

Table 1 Flight Dynamic Equations

The full flight dynamic equations in Table 1 may be linearized into second order differential equations by utilizing small disturbance theory. This theory applies to small deviations (for angle of attack, sideslip and control surface deflections, etc.) relative to some steady state flight condition. For an automatic landing system, this assumption is valid since only small angle deviations caused by turbulence or control variables are encountered. This theory is also useful in analyzing the stability of an autopilot by using longitudinal transfer functions.

Small Perturbation Equations (stability axis)

Perturbed state equations are derived by replacing all motion variables by a steady state value and a perturbation:

$$\begin{aligned}
 U &= U_0 + \Delta U & V &= V_0 + \Delta V & W &= W_0 + \Delta W \\
 P &= P_0 + \Delta P & Q &= Q_0 + \Delta Q & R &= R_0 + \Delta R \\
 \Psi &= \Psi_0 + \Delta \Psi & \Theta &= \Theta_0 + \Delta \Theta & \Phi &= \Phi_0 + \Delta \Phi
 \end{aligned} \tag{45}$$

This also applies to all forces and moments:

$$\begin{aligned}
 F_x &= F_{x_0} + \Delta F_x & F_y &= F_{y_0} + \Delta F_y & F_z &= F_{z_0} + \Delta F_z \\
 M &= M_0 + \Delta M & L &= L_0 + \Delta L & N &= N_0 + \Delta N
 \end{aligned} \tag{46}$$

The change in forces and moments can be expressed in terms of the perturbation variables by using a Taylor series expansion:

$$\begin{aligned}
 \Delta F_x &= \frac{\partial F_x}{\partial U} \Delta U + \frac{\partial F_x}{\partial W} \Delta W + \frac{\partial F_x}{\partial \delta_E} \Delta \delta_E + \frac{\partial F_x}{\partial \delta_T} \Delta \delta_T \\
 \Delta F_y &= \frac{\partial F_y}{\partial V} \Delta V + \frac{\partial F_y}{\partial P} \Delta P + \frac{\partial F_y}{\partial R} \Delta R + \frac{\partial F_y}{\partial \delta_R} \Delta \delta_R \\
 \Delta F_z &= \frac{\partial F_z}{\partial U} \Delta U + \frac{\partial F_z}{\partial W} \Delta W + \frac{\partial F_z}{\partial Q} \Delta Q + \frac{\partial F_z}{\partial \delta_E} \Delta \delta_E + \frac{\partial F_z}{\partial \delta_T} \Delta \delta_T \\
 \Delta M &= \frac{\partial M}{\partial U} \Delta U + \frac{\partial M}{\partial W} \Delta W + \frac{\partial M}{\partial Q} \Delta Q + \frac{\partial M}{\partial \delta_E} \Delta \delta_E + \frac{\partial M}{\partial \delta_T} \Delta \delta_T \\
 \Delta L &= \frac{\partial L}{\partial V} \Delta V + \frac{\partial L}{\partial P} \Delta P + \frac{\partial L}{\partial R} \Delta R + \frac{\partial L}{\partial \delta_R} \Delta \delta_R + \frac{\partial L}{\partial \delta_A} \Delta \delta_A \\
 \Delta N &= \frac{\partial N}{\partial V} \Delta V + \frac{\partial N}{\partial P} \Delta P + \frac{\partial N}{\partial R} \Delta R + \frac{\partial N}{\partial \delta_R} \Delta \delta_R + \frac{\partial N}{\partial \delta_A} \Delta \delta_A
 \end{aligned} \tag{47}$$

The partial derivatives in Equation (47) are called the *stability derivatives*. For convenience, these derivatives are divided by the aircraft mass. These new symbols are defined as *dimensional stability derivatives* (e.g.):

$$X_u = \left(\frac{F_x}{\partial U} \right) / (m) \quad X_w = \left(\frac{F_x}{\partial W} \right) / (m) \tag{48}$$

Replacing the forces and moments with Equation (25) the longitudinal dimensional stability derivatives, in the stability axis system, become:

$$\begin{aligned}
X_u &= \frac{-2C_{D_0}\bar{q}_0S}{mU_0} & X_{\delta_B} &= \frac{-2C_{D_{\delta_B}}\bar{q}_0S}{m} & Z_u &= \frac{-2C_{L_0}\bar{q}_0S}{mU_0} \\
Z_{\dot{\alpha}} &= \frac{-C_{L_{\dot{\alpha}}}\bar{q}_0S\bar{c}}{2mU_0} & Z_q &= \frac{-C_{L_q}\bar{q}_0S\bar{c}}{2mU_0} & Z_{\delta_B} &= \frac{-C_{L_{\delta_B}}\bar{q}_0S}{m} \\
M_u &= \frac{2C_{M_0}\bar{q}_0S\bar{c}}{I_{YY}U_0} & M_\alpha &= \frac{-C_{M_\alpha}\bar{q}_0S\bar{c}}{I_{YY}} & M_{\dot{\alpha}} &= \frac{C_{M_{\dot{\alpha}}}\bar{q}_0S\bar{c}^2}{2I_{YY}U_0} \\
M_q &= \frac{C_{M_q}\bar{q}_0S\bar{c}^2}{2I_{YY}U_0} & M_{\delta_B} &= \frac{C_{M_{\delta_B}}\bar{q}_0S\bar{c}}{I_{YY}} & M_{T_\alpha} &= \frac{C_{M_{T_\alpha}}\bar{q}_0S\bar{c}}{I_{YY}} \\
X_\alpha &= \frac{-(C_{D_\alpha} - C_{L_0})\bar{q}_0S}{m} & Z_\alpha &= \frac{-(C_{L_\alpha} + C_{D_0})\bar{q}_0S}{m}
\end{aligned} \tag{49}$$

These dimensional stability derivatives, along with the force and moment perturbation equations, can now be evaluated into the full flight dynamic equations (Table 1). To simplify the analysis, for small angle deflections, let:

$$\begin{aligned}
\cos \Theta &\approx 1.0 \\
\sin \Theta &\approx \Theta
\end{aligned} \tag{50}$$

Taking a Laplace Transformation of the resulting equations determines the longitudinal transfer functions with the elevator setting (δ_E) as the input and the horizontal velocity component (U), angle of attack (α) and pitch angle (Θ) as the output variables. These longitudinal transfer functions, in matrix form, are:

$$\begin{Bmatrix} A_{11} & A_{12} & A_{13} \\ A_{21} & A_{22} & A_{23} \\ A_{31} & A_{32} & A_{33} \end{Bmatrix} \begin{Bmatrix} \frac{U(s)}{\delta_E(s)} \\ \frac{\alpha(s)}{\delta_E(s)} \\ \frac{\Theta(s)}{\delta_E(s)} \end{Bmatrix} = \begin{Bmatrix} X_{\delta_B} \\ Z_{\delta_B} \\ M_{\delta_B} \end{Bmatrix} \tag{51}$$

where:

$$\begin{aligned}A_{11} &= (s - X_u) \\A_{12} &= -X_\alpha \\A_{13} &= g \cos \Theta_0 \\A_{21} &= -Z_u \\A_{22} &= s(U_0 - Z_{\dot{\alpha}}) - Z_\alpha \\A_{23} &= -(Z_q + U_0)s + g \sin \Theta_0 \\A_{31} &= -(M_u + M_{T_u}) \\A_{32} &= -(sM_{\dot{\alpha}} + M_\alpha) \\A_{33} &= s^2 - sM_q\end{aligned}\tag{52}$$

Taking the inverse of Equation (51) yields the transfer functions for the longitudinal mode. Using Cramer's Rule, the denominator of the transfer functions is a fourth order polynomial. The roots of this polynomial form the *characteristic equation* and determine the stability of an aircraft. The characteristic equation is represented by two oscillatory modes of motion (short period and phugoid).

Short and Long Period Approximations

The longitudinal motion of an aircraft is determined by two modes. The first is the *short period* mode. This is characterized by a highly damped, high natural frequency oscillation at approximately constant speed ($\Delta U \approx 0$). The other mode is the long period or *phugoid* mode. This is caused by a gradual change between potential and kinetic energy and is characterized by a low damped, low natural frequency oscillation at approximately constant angle of attack ($\Delta \alpha \approx 0$). Both modes are determined by the characteristic roots of Equation (51). The concept of these modes is illustrated in Figure 7.

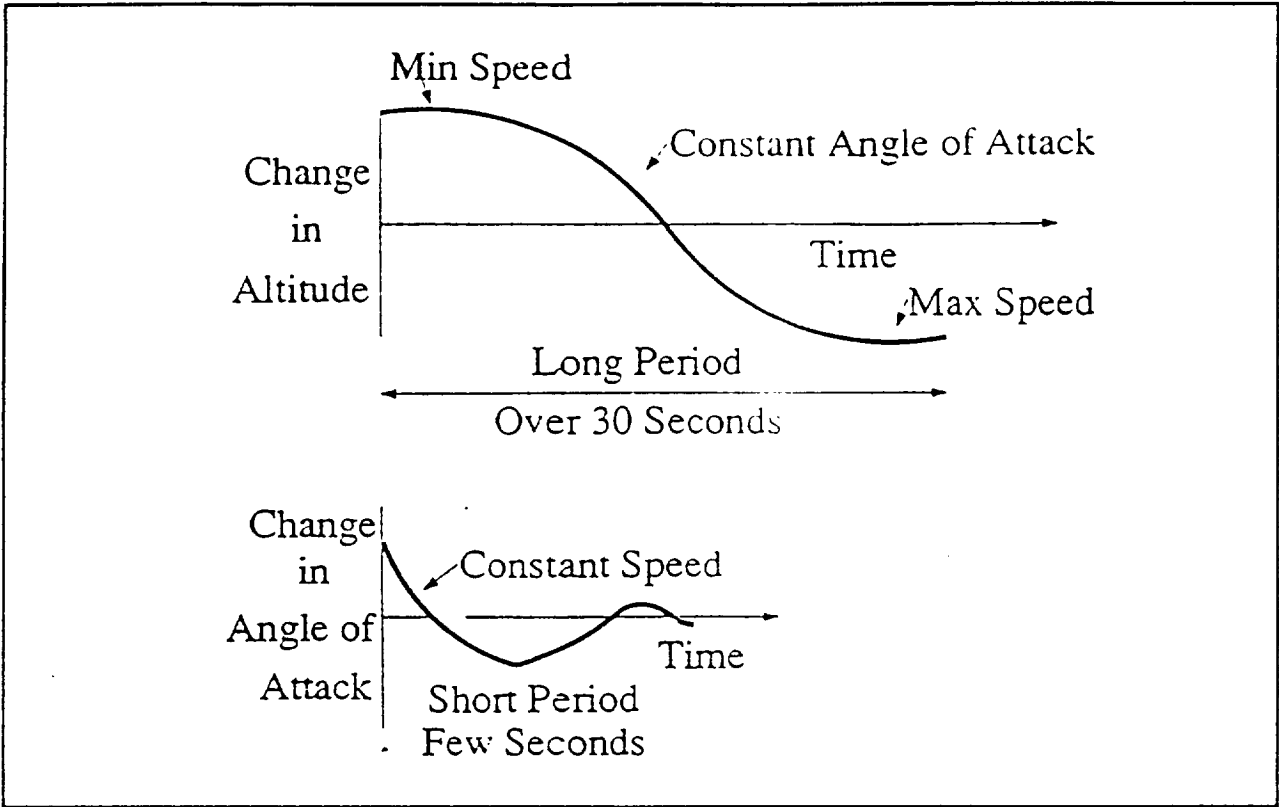


Figure 7 Short Period and Phugoid Modes

The short period mode is obtained by approximately neglecting the velocity term in Equation (51). This equation now reduces to:

$$\begin{Bmatrix} sU_0 - Z_\alpha & -sU_0 \\ -M_{\dot{\alpha}} - M_\alpha & s^2 - sM_q \end{Bmatrix} \begin{Bmatrix} \frac{\alpha(s)}{\delta_E(s)} \\ \frac{\Theta(s)}{\delta_E(s)} \end{Bmatrix} = \begin{Bmatrix} Z_{\delta_E} \\ M_{\delta_E} \end{Bmatrix} \quad (53)$$

Applying the inverse to this equation:

$$\frac{\alpha(s)}{\delta_E(s)} = \frac{sZ_{\delta_E} + (M_{\delta_E}U_0 - M_qZ_{\delta_E})}{s\{s^2U_0 - s(M_qU_0 + Z_\alpha + U_0M_{\dot{\alpha}}) + (Z_\alpha M_q - M_\alpha U_0)\}} \quad (54)$$

$$\frac{\Theta(s)}{\delta_E(s)} = \frac{s(U_0M_{\delta_E} + Z_{\delta_E}M_{\dot{\alpha}}) + (M_\alpha Z_{\delta_E} - Z_\alpha M_{\delta_E})}{s\{s^2U_0 - s(M_qU_0 + Z_\alpha + U_0M_{\dot{\alpha}}) + (Z_\alpha M_q - M_\alpha U_0)\}}$$

Comparing the denominator of this equation to the standard frequency form of $(s^2 + s2\zeta\omega_{n_{SP}} + \omega_{n_{SP}}^2)$, the natural frequency and damping ratio of the short period mode are:

$$\omega_{n_{SP}} = \sqrt{\frac{Z_{\alpha} M_q}{U_0} - M_{\alpha}} \quad (55)$$

$$\zeta_{SP} = \frac{-(M_q U_0 + Z_{\alpha} + M_{\dot{\alpha}} U_0)}{2\omega_{n_{SP}} U_0}$$

The phugoid approximation is derived by neglecting the angle of attack term in Equation (51). The resulting equations for this mode become:

$$\frac{U(s)}{\delta_E(s)} = \frac{Z_{\delta_B} U_0 g}{(s^2 U_0 - s X_u U_0 - Z_u g)} \quad (56)$$

$$\frac{\Theta(s)}{\delta_E(s)} = \frac{-Z_{\delta_B} U_0 (s - X_u)}{(s^2 U_0 - s X_u U_0 - Z_u g)}$$

The natural frequency and damping ratio for the phugoid mode are:

$$\omega_{n_P} = \sqrt{\frac{-Z_u g}{U_0}} \quad (57)$$

$$\zeta_P = \frac{-X_u}{2\omega_{n_P}}$$

The combination of the short period and phugoid modes describes the complete longitudinal aircraft motion (i.e.):

$$\frac{\Theta(s)}{\delta_E(s)} = \frac{k_{\Theta\delta} (T_{\Theta_1} s + 1)(T_{\Theta_2} s + 1)}{\left(\frac{s^2}{\omega_{n_{SP}}^2} + \frac{2\zeta_{SP}}{\omega_{n_{SP}}} + 1\right) \left(\frac{s^2}{\omega_{n_P}^2} + \frac{2\zeta_P}{\omega_{n_P}} + 1\right)} \quad (58)$$

REFERENCES

- [1] Roskam, J., Aircraft Flight Dynamics and Automatic Control, Part I and II, Roskam Aviation and Engineering Corporation, U.S., 1979.
- [2] Nelson, R.C., Flight Stability and Automatic Control, McGraw Hill, 1987.